

P. Lishchuk

Optimized Photoacoustic Gas-Microphone Cell for Semiconductor Materials Thermal Conductivity Monitoring

Taras Shevchenko National University of Kyiv, Kyiv, Ukraine, pavel.lishchuk@univ.kiev.ua

The paper presents the results of the experimental study of thermal transport of semiconductor materials by photoacoustic (PA) gas-microphone (GM) technique. Special attention is paid to the importance of PA cell design and normalization of the informative signal, as necessary conditions for minimizing the extraneous noise or signal caused by both the PA cell geometry and the contribution of electronic components of the experimental set-up. The presented PA technique allows quick and contactless estimating of the semiconductor materials thermal conductivity in a non-destructive way. In particular, the configuration of the PA cell presented in this work allows analyzing the influence of the level of boron doping impurity on the thermal transport of monocrystalline silicon is proposed. The obtained results are in good agreement with the known literature data and are relevant from a practical point of view due to the importance of silicon usage in modern technological applications.

Keywords: photoacoustic gas-microphone method, thermal conductivity, monocrystalline silicon, doped semiconductors.

Received 1 March 2021; Accepted 21 May 2021.

Introduction

The thermal conductivity value is one of the main functional parameters of material science required when dealing with the industrial fabrications of high-efficiency thermoelectric devices and for the desired thermal management of nanostructured semiconductor materials obtained from the investigated bulk wafers [1, 2]. It is worth noting that the peculiarities of thermal transport in solids can be sensitive to a number of factors. Among them are the impurities, dislocations [3], the influence of the different boundaries between the interfaces [4, 5], the presence of the local elastic stresses [6], etc. [7,8]. Therefore, the quite fast and flexible diagnosis of thermal conductivity and related values is significant for studying the nature and checkup the behavior of semiconductor materials before and after various structure manipulations.

Various experimental techniques are successfully applied to study thermal transport in different types of materials. For steady-state thermal methods one should be careful with control of heat losses and temperature fluctuations that may affect the results during the

measurements. The methods with transient or periodic sample heating [9], are also used for the determination of thermal parameters. Among them the main ones are the 3- ω method [10], the laser flash method [11], photoacoustic (PA) technique with piezoelectric [12, 13] and gas-microphone (GM) registration configurations.

The main advantage of PA technique among other methods is its low-cost and flexible unique detection system for various samples that allow non-contact and non-destructive testing and estimating material thermal properties [5,14,15]. Since, the PA response formation is based on the heating of the sample caused by incident electro-magnetic radiation, the usage of PA technique can overcome a typical source of errors characteristic to contact-based thermal measurements. Contrary to GM technique, the thermophysical properties of the material by the piezoelectric method can be performed in vacuum, and in a wider range of temperatures, as well as the modulation frequencies. Nevertheless, the analysis of the PA response for piezoelectric PA method is more complicated and requires the information about the mechanical properties of the sample [16, 17]. Thus, the PA GM technique is one of the most promising methods for

the evaluation of thermal properties of solid homogeneous, layered, or nanostructured materials.

At the same time, it should be emphasized that it is necessary to obtain and take into account the information about the photoacoustic GM cell effects, as well as other sources that potentially affect the behavior of the informative response formation from the sample and its further registration. The purpose of this work is to analyse and interpret information about the physical features of the PA signal formation, and on this basis to optimize the PA GM cell in order to determine the thermal conductivity of semiconductor structures, and, as an example, to demonstrate the effectiveness of this technique to study the contribution of the doping level on the thermal conductivity of monocrystalline silicon (Si).

I. Experimental details

The measurements of PA signal were performed for 3 series of boron-doped p-type (100)-oriented monocrystalline Si samples that vary by the thickness and doping level (see Table 1).

Thermal conductivity measurements of the Si samples were carried out at room temperature. A typical experimental setup of PA method used in this work is shown in Fig. 1. All the samples were alternately placed on the bottom of the inner space of PA cell with built-in electret microphone Panasonic WM61A. Continuous-wave single-mode green laser ($\lambda = 532$ nm) was used as a heating source was modulated by a square signal from AFG1062 Tektronix arbitrary waveform generator. The

by normal filters to the desired values and controlled by laser power meter. The informative signal obtained from the PA cell was compared with the reference one from generator by the lock-in nanovoltmeter Unipan 232B to extract the amplitude of the PA signal. Additionally, an oscilloscope was connected to the interface of the lock-in amplifier for data acquisition and visual control of the experimental details.

A typical PA GM cell is realised as a small container for the sample under study with mounted optically transparent window and a microphone for registration of the thermally induced pressure changes inside the inner gaseous space of the cell during the non-stationary irradiation of sample surface. Both the optimal design of the PA cell and its calibration represent a crucial point for the success in thermal properties measurements of solids [18, 19]. The PA cell used in this work was made from aluminum that have an extremely weak optical absorption for the laser beam used, and have an inner space volume of $16 \times 8 \times 3.1 \text{ mm}^3$, where 3.1 mm is a “baking material – to – window” distance. Compared with existing PA cell counterparts [20-23], the proposed GM cell configuration is optimal for thermal conductivity study of the samples taking into account the following important factors:

- PA signal amplitude is inversely proportional to inner volume of PA cell;
- the inner space reduction of the PA cell should be limited by the dimension of the electret microphone;
- samples are analyzed in a non-contact non-destructive manner;
- the ability to simultaneously place a sample for research and reference material with well-established

Table 1

Characteristics of the investigated Si samples

Sample №	Thickness, μm	Doping level, cm^{-3}	Density, kg/m^3	Heat capacity, $\text{J}/(\text{kg K})$
1	515	$10^{19}\text{-}10^{20}$	2330	680
2	440	$10^{19}\text{-}10^{20}$		
3	260	10^{15}		

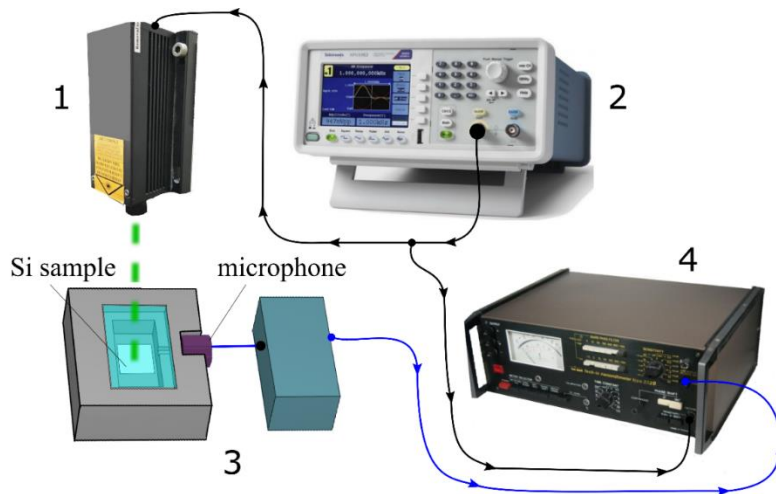


Fig. 1. Schematic view of the main components of experimental set-up: 1 – 532 nm laser, 2 – waveform generator, 3 – PA GM cell with phantom power supply, 4 – lock-in nanovoltmeter.

initial output optical power of laser 500 mW was reduced

properties in the cell should be realized (the area of each

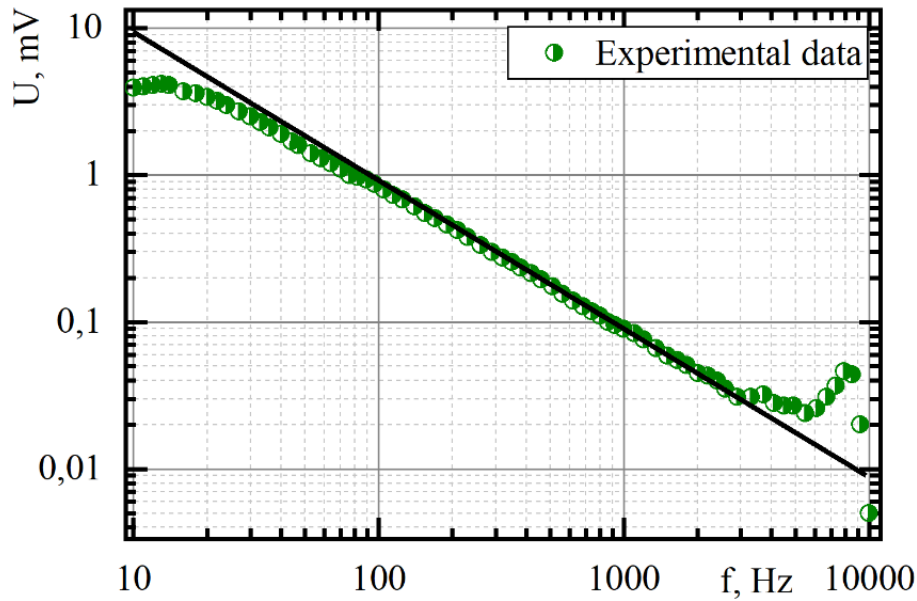


Fig. 2. Experimental PA AFC obtained for reference black carbon sample during its irradiation by green laser with output power 72 mW. The solid line represents the theoretical dependence predicted by the Rosencwaig and Gersho model [24] for carbon sample. The error of the experimentally obtained frequency response is within the points shown on the graph (here and in the following figures).

sample mounted in the proposed PA cell can reach $8 \times 8 \text{ mm}^2$);

- the dimensions of the cell should be made to minimize the contribution of the effect of the PA cell walls and window acting as possible heat sinks on the informative signal;

- it is necessary to shift the resonant frequencies of the cell as far away from the operating frequencies as possible to study the thermal properties of the samples.

The $515 \text{ }\mu\text{m}$ homogeneous black carbon was used as a reference sample for calibration of PA cell to remove the possible additional parasitic signals during the main experiments (see Fig. 2).

According to the one-dimensional model proposed by the Rosencwaig and Gersho [24], it could be predicted that the amplitude-frequency characteristics (AFC) for thermally thick high-absorbing reference sample should have a constant slope of «-1» while increasing the modulation frequency. However, the observed AFC behavior differs markedly from the theoretical one at both high and low frequencies.

The deviation of experimental results from the theory at low frequencies can have a number of reasons. In this case, the PA signal may include the contribution from effects that are related to the PA cell instrumental factors (heat-sink effects, optical properties of PA cell material, etc.), as well, as the microphone used (sensitivity losses, measurement-damaging design features for the microphone durability, etc.) and the electrical circuits of measuring equipment.

On the other hand, even a simple PA cell exhibits its own acoustic resonances that mainly depend on its characteristic dimensions. Other possible sources of the resonance like a diaphragm of the detector microphone should not be ruled out. Moreover, increasing the modulation frequency results in a signal-to-noise ratio

decreasing. Thus, any experimental measurement of PA response should be carefully analyzed and calibrated before the fitting procedure by the theoretic model, especially at both the low and high frequencies.

It should be noted that the calibration coefficients from measurements of black carbon at different laser irradiation powers and the height of the calibration sample correlate well enough and can be used for normalization of PA signal obtained from Si samples. However, the small-amplitude difference of PA response caused by the extra volume appearance inside the PA cell if we place a smaller sample should be also taken into account.

II. Results and discussion

In this work the measurements of the PA signal generated by the Si sample's irradiation with output optical power 145 mW were performed in non-resonant frequency range – from 10 Hz to 1500 Hz (see Fig. 3). For analysis of the obtained experimental results, a thermal wave formalism was used [25]. Due to this approach, the excited by non-stationary light thermal perturbation can be represented as a rapidly damped heat wave that can be characterized by the following equation:

$$\lambda_T = \sqrt{D_T / (\pi f)}, \quad (1)$$

where λ_T , - the thermal wave wavelength, D_T - the thermal diffusivity of the sample, f - the modulation frequency, respectively.

Thus, in case when for Si sample with a thickness l_{Si} a characteristic frequency (“bending frequency”), at which $\lambda_T \sim l_{Si}$ belong to the diapason of frequencies under investigation, as a result this frequency will divide the

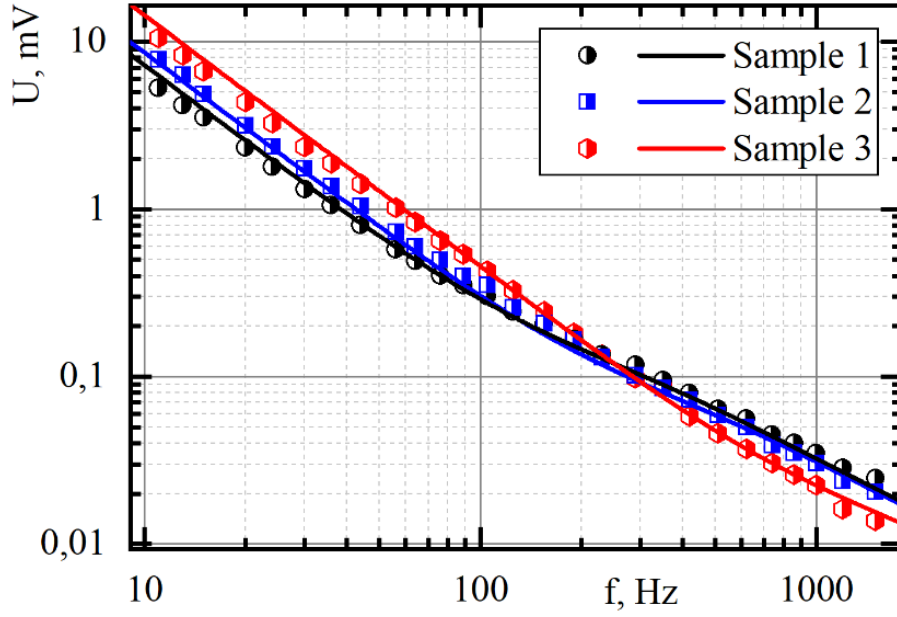


Fig. 3. Normalized experimental results (dots) of the AFC of PA response formation from the Si samples, treated by model calculations (represented by lines).

Table 2

Comparative characteristics of experimentally obtained thermal conductivity values of the Si samples with findings from the literature.

Sample	K, W/(m K)		
	Based on bending frequency analysis	Obtained by model calculations	Literature data [26, 27]
1	102 ± 9	100 ± 10	110
2	114 ± 8	110 ± 10	110
3	133 ± 8	130 ± 10	130

AFC of the PA response into the low-frequency and high-frequency regions that differ by the slope of the function. The high-frequency region that is above bending at a certain frequency corresponds to the situation when $\lambda_T < l_{Si}$, and implies that thermal perturbation is localized within the Si sample.

On the other hand, for low modulation frequencies, the value of the wavelength is more than l_{Si} and, thus, the thermal perturbation behavior on the bottom Al side of the PA cell that is in thermal contact with the sample will also influence the PA signal formation. Thereby, the experimental evaluation of such a bending frequency allows one to obtain thermal conductivity of Si sample $K_{Si} = D_T c_{Si} \rho_{Si}$ from the following expression:

$$K_{Si} = \pi f_b l_{Si}^2 \rho_{Si} c_{Si} .(2)$$

where f_b is the bending frequency, c_{Si} is the specific heat of Si sample, ρ_{Si} is the density of Si sample, respectively.

Thus, the observed in AFC bending frequencies (78 ± 6) Hz for Sample 1, (118 ± 5) Hz for sample 2, (390 ± 15) Hz for Sample 3, allow to obtain the corresponding thermal conductivities (see Table. 2). To simplify the calculations, an approximation was taken into account,

according to which the doping level of impurity does not affect the volumetric heat capacity of the samples. ($\rho_{Si} c_{Si}$).

The approach presented above explains the behavior of the PA AFC slopes on a double logarithmic scale and allows one to find the thermal conductivity of the sample. Nevertheless, more precise analysis of the obtained AFCs is based on the calculation of the variable temperature component (θ) distribution in one-dimensional approximation according to the following equation, as described earlier in [28, 29]:

$$\frac{d^2\theta}{dz^2} - \frac{2\pi f c \rho i}{K} = I_0(1 - R)\alpha \cdot \exp(-az), \quad (3)$$

where K , c , and ρ are the thermal conductivity, heat capacity and density of the sample, respectively; I_0 is the intensity of absorbed light; R , and α are the reflectivity and absorption coefficient of the sample at the considered wavelength of irradiation source, respectively.

Considering the adiabatic boundary conditions the pressure fluctuations inside PA cell can be evaluated as follows:

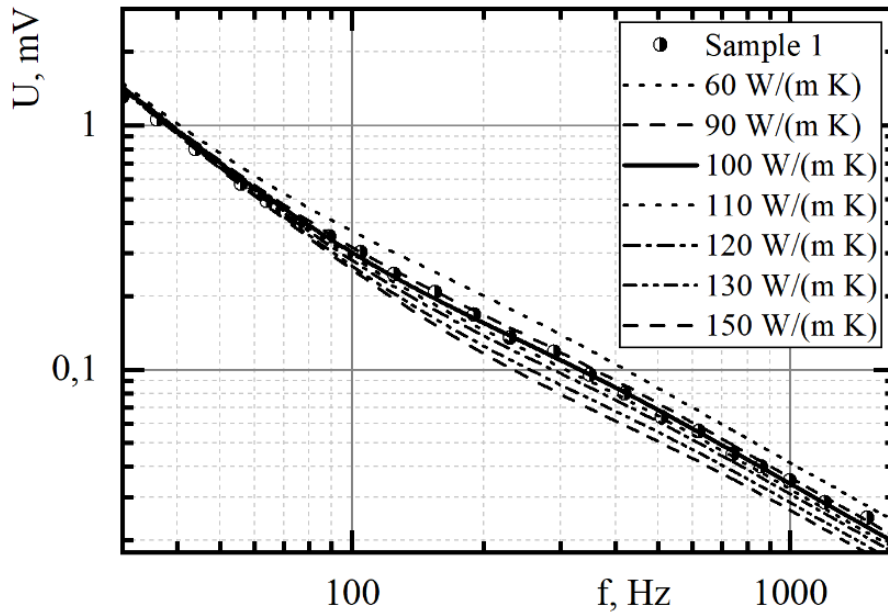


Fig. 4. Amplitude-frequency dependencies for different values of thermal conductivity, calculated for Sample 1. Experimental results represented by dots.

$$\rho(f) \sim \int_0^{\infty} \theta(f, z) dz = -\theta(0) \sqrt{\frac{K_{gas}}{i 2\pi f c_{gas} \rho_{gas}}} \quad (4)$$

where $\theta(0)$ – is the temperature on the surface of the sample, K_{gas} , c_{gas} , ρ_{gas} are the thermal conductivity, heat capacity and density of the isolated gas (air).

Taking into account the known laser irradiation power, volumetric heat capacity and optical absorption coefficient of monocrystalline silicon at a wavelength of 532 nm [30], the thermal conductivity of the samples can be calculated by varying its value to achieve the maximum possible correlation between the experimentally obtained AFC of the PA signal and theoretically calculated with finite difference method based on equation (4) (see Fig. 4). Informative markers for the approximation procedure are the amplitude and change of the inclination angle of the experimentally obtained AFC of PA response.

The obtained thermal conductivity values when the experimental and theoretical results qualitatively correlate with each other for each series of samples (see Fig. 3), are shown in Table 2. Therefore, the calculated coefficients of thermal conductivity of the studied samples using both approaches are in a good agreement with the known reference data from literature [26, 27].

Conclusion

The paper presents the thermal conductivity evaluation of semiconductor materials by means of the photoacoustic gas-microphone technique. It is shown that the method requires a carefully constructed photoacoustic

cell with sensitive and precisely manufactured components. It has been proven that the calibration process of the photoacoustic signal from a material with known thermophysical properties in the manufactured cell is an important first step before providing a study of the photoacoustic response from the samples. To determine thermal conductivity values of the studied samples, a comprehensive methodology to the analysis of the frequency response of the amplitude of the photoacoustic signal based on the thermal wave approach is proposed. In particular, it was used to study the thermal conductivity dependence of silicon wafers on the boron doping level. It is shown that the obtained results are in good agreement with the literature data. Thus, the presented configuration of the photoacoustic cell allows studying the features of thermal transport of a wide range of semiconductor materials in a cheap, quick and contactless non-destructive way.

Acknowledgements

I want to acknowledge the financial support of the Ministry of Education and Science of Ukraine through the project “Features of photothermal and photoacoustic processes in low-dimensional silicon-based semiconductor systems” (State registration number 0118U000242) and Dr. Mykola Isaiev from the Université de Lorraine, CNRS, LEMTA (Nancy, France) for his interest in this work and helpful discussions.

Lishchuk P. - Ph.D., Assistant Professor of General Physics Department.

- [1] L. Canham, *Handbook of Porous Silicon* Leigh Canham Springer, 2015 <http://www.springer.com/us/book/9783319057439%5Cnfiles/197/9783319057439.html>.
- [2] M. Lee, *J. Supercond. Nov. Magn.* 33, 253 (2020) <https://doi.org/10.1007/s10948-019-05268-5>.
- [3] K. Termentzidis, M. Isaiev, A. Salnikova, I. Belabbas, D. Lacroix, J. Kioseoglou, *Phys. Chem. Chem. Phys.* 20, 5159 (2018) <https://doi.org/10.1039/C7CP07821H>.
- [4] P. Lishchuk, A. Dekret, A. Pastushenko, A. Kuzmich, R. Burbelo, A. Belarouci, V. Lysenko, M. Isaiev, *Int. J. Therm. Sci.* 134, 317 (2018) <https://doi.org/10.1016/j.ijthermalsci.2018.08.015>.
- [5] K. Dubyk, L. Chepela, P. Lishchuk, A. Belarouci, D. Lacroix, M. Isaiev, *Appl. Phys. Lett.* 115, 021902 (2019) <https://doi.org/10.1063/1.5099010>.
- [6] V. Kuryliuk, O. Nepochatyi, P. Chantrenne, D. Lacroix, M. Isaiev, *J. Appl. Phys.* 126, 055109 (2019) <https://doi.org/10.1063/1.5108780>.
- [7] K. Dubyk, T. Nychporuk, V. Lysenko, K. Termentzidis, G. Castanet, F. Lemoine, D. Lacroix, M. Isaiev, *J. Appl. Phys.* 127 (2020) 225101. <https://doi.org/10.1063/5.0007559>.
- [8] M. Isaiev, X. Wang, K. Termentzidis, D. Lacroix, *Appl. Phys. Lett.* 117, 033701 (2020) <https://doi.org/10.1063/5.0014680>.
- [9] R. Burbelo, D. Andrusenko, M. Isaiev, A. Kuzmich, *Arch. Met. Mater.* 56, 1157 (2011) <https://doi.org/10.2478/v10172-011-0129-2>.
- [10] H. Wang, M. Sen, *Int. J. Heat Mass Transf.* 52, 2102 (2009) <https://doi.org/10.1016/j.ijheatmasstransfer.2008.10.020>.
- [11] M. Ruoho, K. Valset, T. Finstad, I. Tittonen, *Nanotechnology* 26, 195706 (2015) <https://doi.org/10.1088/0957-4484/26/19/195706>.
- [12] S. Alekseev, D. Andrusenko, R. Burbelo, M. Isaiev, A. Kuzmich, *J. Phys. Conf. Ser.* 278, 012003 (2011) <https://doi.org/10.1088/1742-6596/278/1/012003>.
- [13] K. Dubyk, A. Pastushenko, T. Nychporuk, R. Burbelo, M. Isaiev, V. Lysenko, *J. Phys. Chem. Solids* 126, 267 (2019) <https://doi.org/10.1016/j.jpics.2018.12.002>.
- [14] M. Isaiev, P.J. Newby, B. Canut, A. Tytarenko, P. Lishchuk, D. Andrusenko, S. Gomès, J.-M. Bluet, L.G. Fréchet, V. Lysenko, R. Burbelo, *Mater. Lett.* 128, 71 (2014) <https://doi.org/10.1016/j.matlet.2014.04.105>.
- [15] M. Isaiev, S. Tutashkonko, V. Jean, K. Termentzidis, T. Nychporuk, D. Andrusenko, O. Marty, R.M. Burbelo, D. Lacroix, V. Lysenko, *Appl. Phys. Lett.* 105, 031912 (2014) <https://doi.org/10.1063/1.4891196>.
- [16] D. Andrusenko, M. Isaiev, A. Kuzmich, V. Lysenko, R. Burbelo, *Nanoscale Res. Lett.* 7, 1 (2012) <https://doi.org/10.1186/1556-276X-7-411>.
- [17] M. Isaiev, D. Andrusenko, A. Tytarenko, A. Kuzmich, V. Lysenko, R. Burbelo, *Int. J. Thermophys* (2014) <https://doi.org/10.1007/s10765-014-1652-y>.
- [18] R.W. Jones, J.F. McClelland, *Appl. Spectrosc.* 55, 1360 (2001) (<https://doi.org/10.1366/0003702011953487>).
- [19] X. Wang, B. Cola, T. Bougher, S. Hodson, T. Fisher, X. Xu, *Annu. Rev. Heat Transf.* (2012) <https://doi.org/10.1615/AnnualRevHeatTransfer.2012004780>.
- [20] S. Alekseev, D. Andrusenko, R. Burbelo, M. Isaiev, a Kuzmich, *J. Phys. Conf. Ser.* 278, 012003 (2011) <https://doi.org/10.1088/1742-6596/278/1/012003>.
- [21] D. Andrusenko, M. Isaiev, A. Tytarenko, V. Lysenko, R. Burbelo, *Microporous Mesoporous Mater.* 194, 79 (2014) <https://doi.org/10.1016/j.micromeso.2014.03.045>.
- [22] J. Pelzl, K. Klein, O. Nordhaus, *Appl. Opt.* 21, 94 (1982) <https://doi.org/10.1364/AO.21.000094>.
- [23] Q. Shen†, T. Takahashi, T. Toyoda, *Anal. Chem.* 73, 281 (2001).
- [24] A. Rosencwaig, A. Gersho, *J. Appl. Phys.* 47, 64 (1976) <https://doi.org/10.1063/1.322296>.
- [25] P. Lishchuk, D. Andrusenko, M. Isaiev, V. Lysenko, R. Burbelo, *Int. J. Thermophys.* 36, 2428 (2015) <https://doi.org/10.1007/s10765-015-1849-8>.
- [26] M. Asheghi, K. Kurabayashi, R. Kasnavi, K.E. Goodson, *J. Appl. Phys.* 91, 5079 (2002) <https://doi.org/10.1063/1.1458057>.
- [27] M.G. Burzo, P.L. Komarov, P.E. Raad, Non-contact thermal conductivity measurements of p-doped and n-doped gold covered natural and isotopically-pure silicon and their oxides, in: *5th Int. Conf. Therm. Mech. Simul. Exp. Microelectron. Microsystems, 2004. EuroSimE 2004. Proc., IEEE, (2004). P. 269.* <https://doi.org/10.1109/ESIME.2004.1304050>.
- [28] P. Lishchuk, M. Isaiev, L. Osminkina, R. Burbelo, T. Nychporuk, V. Timoshenko, *Phys. E Low-Dimensional Syst. Nanostructures* 107, 131 (2019) <https://doi.org/10.1016/j.physe.2018.11.016>.
- [29] A.I. Tytarenko, D.A. Andrusenko, A.G. Kuzmich, I.V. Gavril'chenko, V.A. Skryshevskii, M.V. Isaiev, R.M. Burbelo, *Tech. Phys. Lett.* 40, 188 (2014) <https://doi.org/10.1134/S1063785014030146>.
- [30] M.A. Green, *Sol. Energy Mater. Sol. Cells.* 92, 1305 (2008) <https://doi.org/10.1016/j.solmat.2008.06.009>.

П.О. Ліщук

Оптимізована фотоакустична газомікрофонна комірка для контролю теплопровідності напівпровідникових матеріалів

Київський національний університет імені Тараса Шевченка, Київ, Україна, pavel.lishchuk@univ.kiev.ua

В роботі представлено результати дослідження особливостей теплового транспорту напівпровідникових матеріалів фотоакустичним (ФА) газомікрофонним (ГМ) методом. Акцентується увага на важливості проектування ФА ГМ комірки та нормування інформативного сигналу, як необхідних умов мінімізації паразитних сигналів, спричиненими як особливостями геометрії ФА комірки, так і внеском від електронних компонентів експериментального стенду. Представлена ФА методика дозволяє швидко та безконтактно неруйнівним способом оцінювати значення коефіцієнту теплопровідності напівпровідникових матеріалів. Зокрема, в рамках даної роботи пропонується конфігурація ФА комірки, яка дозволяє проводити аналіз впливу рівня легуючої домішки бору на особливості теплового транспорту монокристалічного кремнію. Отримані результати добре узгоджуються з відомими літературними даними та є актуальними з практичної точки зору, оскільки розуміння теплового транспорту у таких структурах є важливим аспектом їх використання в сучасних технологічних застосуваннях.

Ключові слова: фотоакустичний газомікрофонний метод, коефіцієнт теплопровідності, монокристалічний кремній, леговані напівпровідники.